

A SHALLOW LAYERED STRUCTURE AT CHANG'E-4 LANDING SITE REVEALED USING LUNAR PENETRATING RADAR. I. Giannakis¹, F. Zhou², C. Warren³ and A. Giannopoulos⁴. ¹School of Geosciences, University of Aberdeen, Meston Building, Kings College, Aberdeen, UK, AB24 3FX. e-mail: iraklis.giannakis@abdn.ac.uk, ²China University of Geosciences, School of Mechanical Engineering and Electronic Information, Wuhan, China, 388 Lumo Rd, Hongshan. e-mail: zhoufeng617@aliyun.com, ³Department of Mechanical and Construction Engineering, Northumbria University, Newcastle, UK, NE1 8ST, e-mail: craig.warren@northumbria.ac.uk, ⁴School of Engineering, The University of Edinburgh, Edinburgh, EH9 3FG, UK. e-mail: a.giannopoulos@ed.ac.uk.

Introduction: Ground Penetrating Radar (GPR) -or as referred to Lunar sciences, Lunar Penetrating Radar (LPR)- is a mature methodology that has been extensively applied to various areas of near surface and environmental geophysics. For planetary sciences, GPR has been used both for satellite [1] and in situ [2] configurations. The Chang'E-3 and E-4 were the first missions that utilized common-offset in-situ GPR data for inferring the dielectric properties of the Lunar ejecta [2]. Within that context, hyperbola-fitting is the most mainstream tool applied for inferring the electric permittivity of subsurface Lunar materials and subsequently estimating their density using semi-empirical models derived from the Apollo samples [3]. Traditional hyperbola-fitting assumes a homogenous half-space, which limits its applicability to non-homogenous layered media. In the current paper, we suggest a novel interpretation tool that assumes that electric permittivity varies arbitrary with respect to depth. Using this method, a previously unseen layered structure is revealed at the first ~12 m of the Von Kármán (VK) crater at Chang'E-4 landing site; and a new stratigraphic model is suggested based on these new evidences.

Methodology: For a target located at $\mathbf{A} = \langle x_0, d \rangle$ inside a homogenous medium with relative electric permittivity ϵ ; and an antenna located at $\mathbf{B} = \langle x, y \rangle$, the two-way arrival time equals with $t = \frac{2}{c_0} \sqrt{\epsilon} (\|\mathbf{A} - \mathbf{B}\|)$, where $c_0 \approx 3 \times 10^8 \text{ m/s}$ is the speed of light in vacuum and t is the two-way first arrival time measured in seconds [3]. It can be proven, that the two-way arrival times will form a hyperbola with an apex at $[x_0, t_0]$ [3]. The depth of the target can be estimated via $d = \frac{c_0 t_0}{2\sqrt{\epsilon}}$ and therefore, the position of the target can be re-written as $\mathbf{A} = \langle x_0, \frac{c_0 t_0}{2\sqrt{\epsilon}} \rangle$. Typical hyperbola fitting, tries to find the optimum permittivity value that minimizes the error $\min_{\epsilon \in \mathbb{R}} \mathbf{t} - \mathbf{T}$, where the vectors \mathbf{t} and \mathbf{T} are the measured and simulated two-way arrival times [3]. It will be shown in the next section, that this strategy leads to unreliable results when applying to layered media that deviate from the underlying assumptions i.e. homogenous half space. To mitigate that, we suggest a novel hyperbola fitting

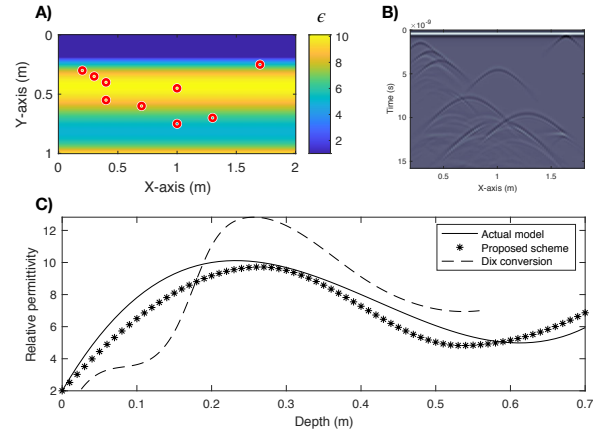


Figure 1: A) The investigated numerical case study. Nine targets are buried in a layered medium with smooth boundaries. B) The resulting radagram; notice that no reflections occur from the layers due to the smooth boundaries between them. C) The reconstructed permittivity profile using typical hyperbola-fitting with Dix conversion and the proposed scheme.

scheme that takes into account the variations of permittivity with respect to depth (y). Within that context, the two-way arrival time equals with $t = \frac{2}{c_0} \int_0^1 \sqrt{\epsilon(y)} \left\| \frac{dq(m)}{dm} \right\| dm$, where $q(m)$ ($m \in [0,1]$) is the path that the wave will travel from point \mathbf{B} to point \mathbf{A} . It is proven (in the next section) that assuming a linear path does not compromise the accuracy of the results; and it leads to an elegant and computationally efficient scheme. Therefore, for $q(m) = \mathbf{A} + (\mathbf{B} - \mathbf{A})m$, and after some algebraic manipulations, we derive $t = \frac{2\|\mathbf{A}-\mathbf{B}\|}{c_0 d} \int_0^d \sqrt{\epsilon(y)} dy$ which can be solved numerically via $t = \frac{2\|\mathbf{A}-\mathbf{B}\|}{c_0 d} \sum_{s=0}^Q \sqrt{\epsilon(s \cdot \Delta y)} \Delta y$, where $Q = d/\Delta y$ and Δy is the discretization step. The depth d can be calculated from the apex of each hyperbola using the bisection method. To further simplify the problem, the permittivity $\epsilon(y)$ is approximated with a spline interpolation between N equidistant points. The novel hyperbola-fitting scheme utilizes Z number of targets to find the optimum N permittivity values that simultaneously minimize $\sum_{i=1}^Z \min_{\epsilon(1), \epsilon(2), \dots, \epsilon(N)} \mathbf{t}_i - \mathbf{T}_i$. Via this approach, a permittivity profile can be derived that

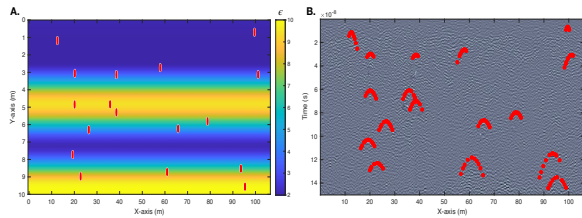


Figure 2: A) The reconstructed permittivity profile of the Chang'E-4 landing site. Red circles correspond to the targets used for the inversion. B) The processed radagram and the fitted hyperbolas for the reconstructed permittivity profile.

can reveal layers that were previously unseen using typical hyperbola-fitting and reflection-based interpretation strategies.

Numerical results: The proposed methodology is tested on the numerical case study illustrated in Figure 1_A. Nine targets are buried in a layered medium consisting of four distinct layers with a permittivity that varies from $\epsilon \in [2 - 10]$. From Figure 1_B, it is apparent, that the layers are not visible in the resulting radagram. This is due to the smooth boundaries between the layers that reduce their reflection coefficients making them “transparent” to electromagnetic waves. The shapes of the hyperbolas are the only features that can be used to infer the subsurface dielectric structure.

Figure 1_C shows the results using typical hyperbola-fitting (complemented with Dix conversion) and the proposed methodology. The proposed scheme over-performs typical hyperbola-fitting and manages to accurately reconstruct the permittivity profile of the investigated medium.

Chang'E-4 GPR data: The suggested scheme is applied to the data collected by the high frequency antenna mounted at Yutu-2 rover during the first two Lunar days of the Chang'E-4 mission [2]. We focus on the first 150 ns of the radagram to infer the layered structure (if any) of the first ~10-12 m of the ejecta. Previous approaches, concluded that the first ~12 m consists of a homogenous weathered regolith overlaying the ejecta from the Finsen crater [2].

Figure 2 illustrates the employed radagram and the resulting permittivity profile using the proposed methodology. A previously unseen layered structure is revealed with relative permittivity that varies from $\epsilon \in [2 - 10]$. This interpretation deviates from previous theories indicating a more complex stratigraphy for the first ~12 meters.

Stratigraphic model: The previously suggested ~12 m weathered layer [2] is not in good agreement with LROC NAC images [4] and by the layered structure revealed by the proposed interpretation scheme (Figure 2). We suggest that the top 10-12 m of

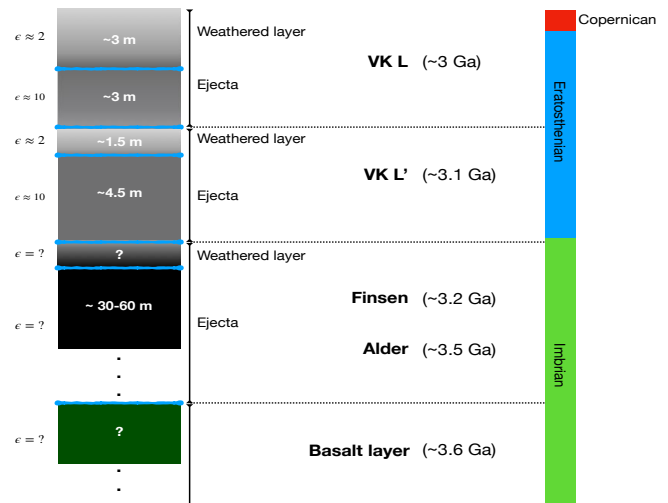


Figure 3: The proposed stratigraphic model for the shallow Lunar ejecta at the Chang'E-4 landing site based on the results illustrated at Figure 2.

the landing site are part of the ejecta from the VK L and L' craters overlaying the Finsen ejecta. This is in good agreement with the Mg-rich and low Ca-pyroxene content of the VK L and L' craters [4] and with the layered structure illustrated in Figure 2. The ejecta of VK L' (~ 5.5 m) were deposited on top of the Finsen ejecta at early Eratosthenian. Space weathering degraded the first ~1.5 m of the ejecta decreasing its density and electric permittivity. The width of the VK L' regolith is in good agreement with the rapid weathering that is expected at young ejecta [5]. The ejecta from VK L were subsequently deposited on top of the weathered layer creating a top layer with ~6 m width. The long weathering process, from early Eratosthenian till now, gave rise to a ~3 m of loose Lunar soil with low electric permittivity. This is in good agreement with the LROC NAC images [4] and with the average weathering rate (~1.5 m/Ga) derived from the Apollo missions [5].

Conclusions: A novel interpretation tool using LPR is presented. The superiority of this approach compared to traditional hyperbola-fitting is showed via numerical simulations. The proposed methodology is subsequently applied to the LPR data from the Chang'E-4 mission. A previously unseen layered structure for the first ~10-12 m is revealed. Based on that, a new stratigraphic model is suggested that is consistent with the chemical composition of the ejecta and the expected Lunar weathering rates.

References: [1] Lauro S. E. et al. (2020) *Nature Astronomy*. [2] Zhang L. et al. (2020), *Geophysical Research Letters*, 47. [3] Dong Z. et. al. (2020) *Geophysical Research Letters*, 47. [4] Huang J. et al. (2018), *Journal of Geophysical Research: Planets*, 123. [5] Gou S. et al. (2021), *Icarus*, 354, 114046.